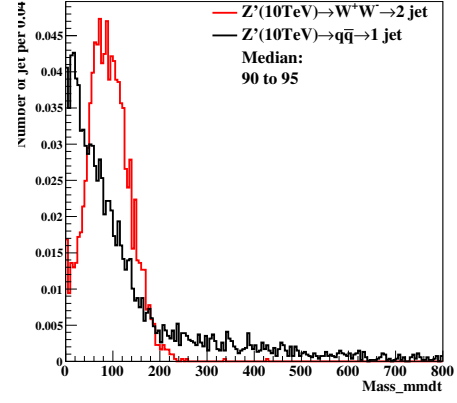
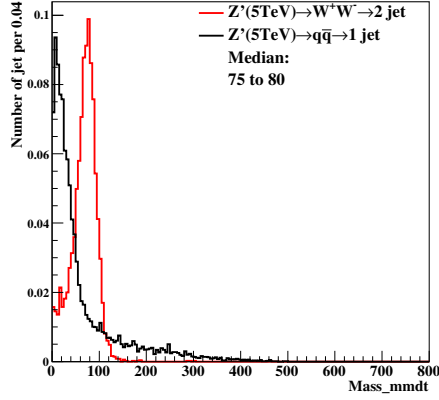


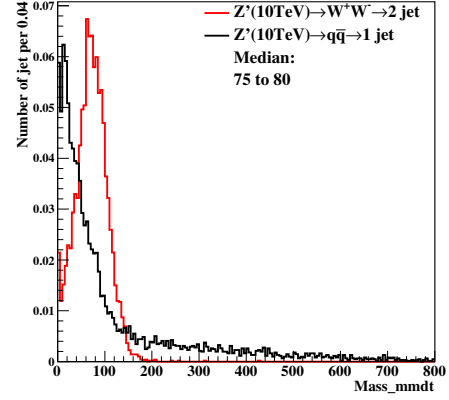
(a) 5TeV at 20×20 (cm \times cm) in cluster



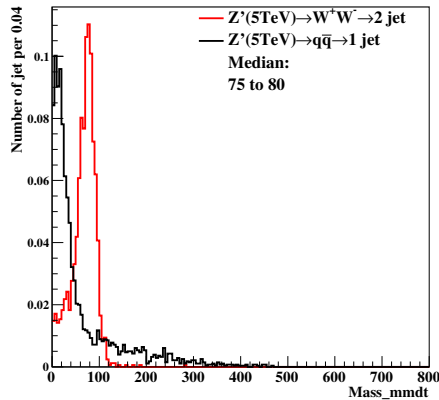
(b) 10TeV at 20×20 (cm \times cm) in cluster



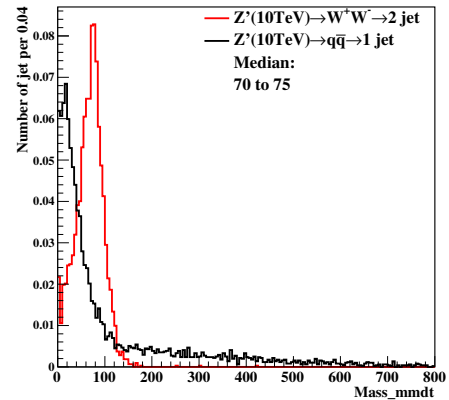
(c) 5TeV at 5×5 (cm \times cm) in cluster



(d) 10TeV at 5×5 (cm \times cm) in cluster

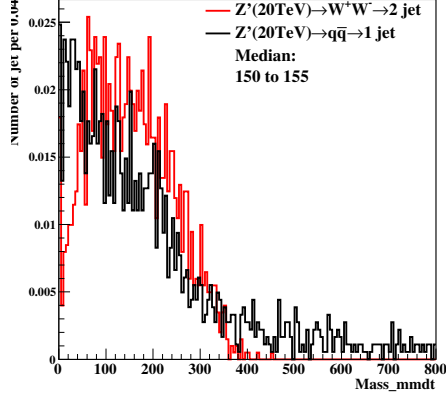


(e) 5TeV at 1×1 (cm \times cm) in cluster

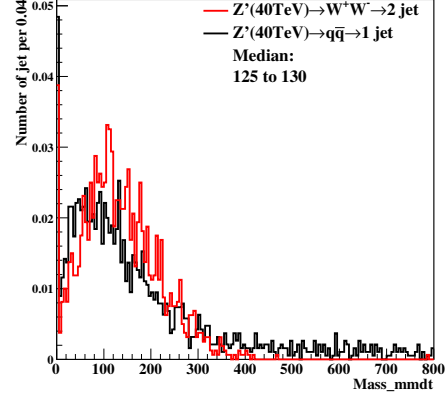


(f) 10TeV at 1×1 (cm \times cm) in cluster

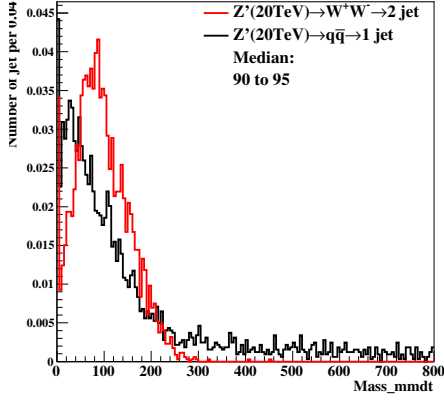
Figure 1: Distributions of mass soft drop at $\beta=0$, signal=ww, in 5,10TeV energy of collision in different detector sizes. Cell Size in 20×20 , 5×5 , and 1×1 (cm \times cm) are shown here.



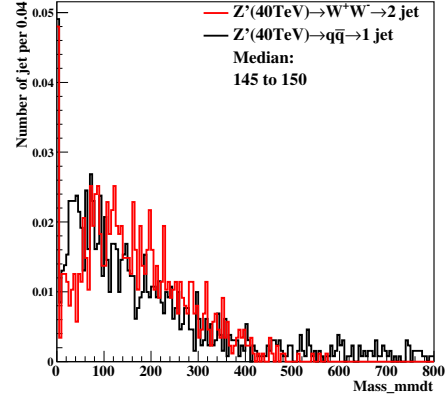
(a) 20TeV at 20×20(cm×cm) in cluster



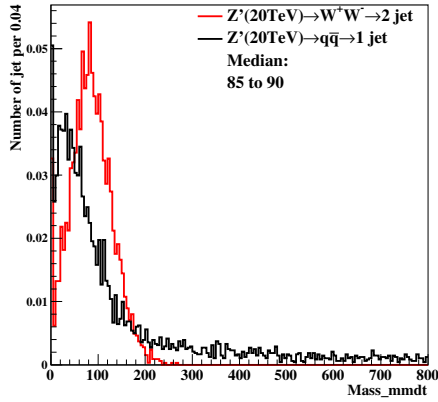
(b) 40TeV at 20×20(cm×cm) in cluster



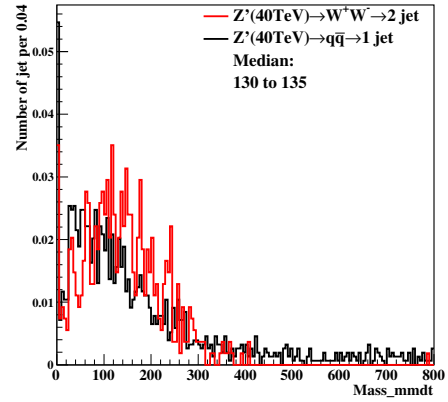
(c) 20TeV at 5×5(cm×cm) in cluster



(d) 40TeV at 5×5(cm×cm) in cluster

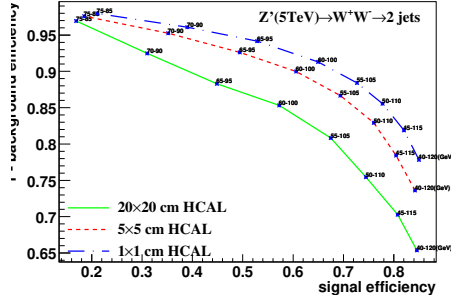


(e) 20TeV at 1×1(cm×cm) in cluster

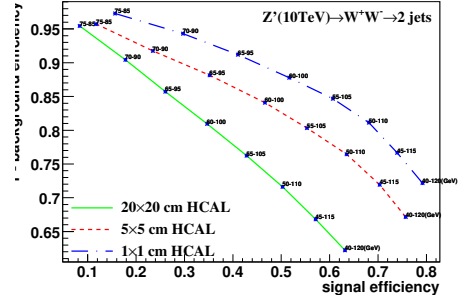


(f) 40TeV at 1×1(cm×cm) in cluster

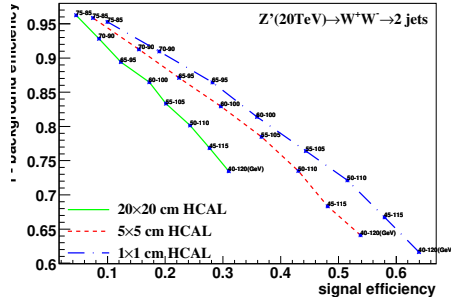
Figure 2: Distributions of mass soft drop at $\beta=0$, signal=ww, in 20,40TeV energy of collision in different detector sizes. Cell Size in 20×20, 5×5, and 1×1(cm×cm) are shown here.



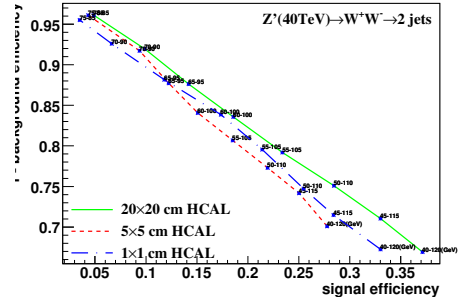
(a) Central at 80TeV change width in cluster at 5TeV



(b) Central at 80TeV change width in cluster at 10TeV

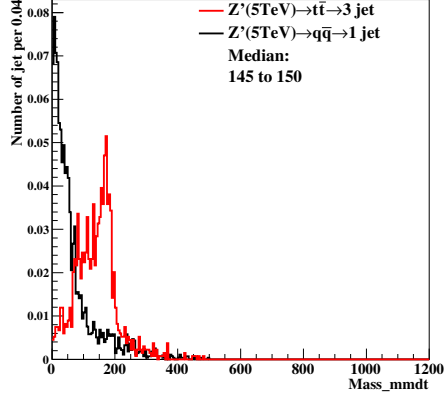


(c) Central at 80TeV change width in cluster at 20TeV

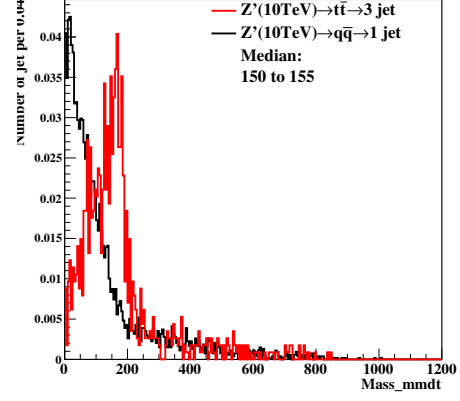


(d) Central at 80TeV change width in cluster at 40TeV

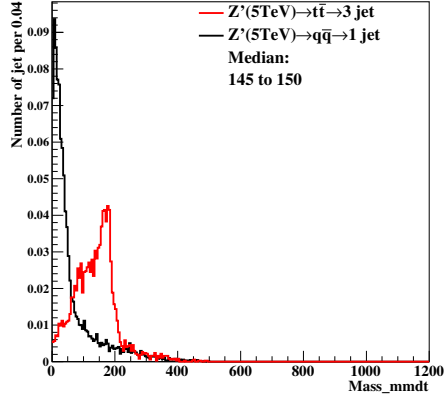
Figure 3: study of "fix central and change width" in mass soft drop at $\beta=0$, signal=ww, in 5, 10, 20, 40TeV energy of collision in different detector sizes. Cell Size in 20x20, 5x5, and 1x1(cmxcn) are shown in each picture.



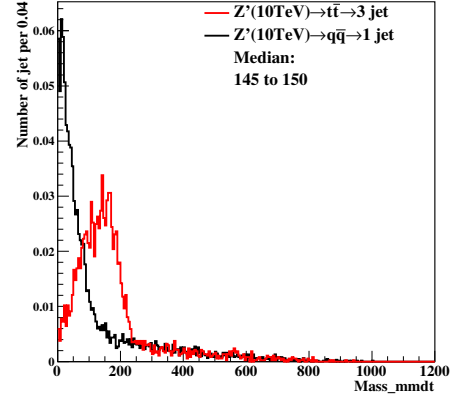
(a) 5TeV at 20×20 (cm \times cm) in cluster



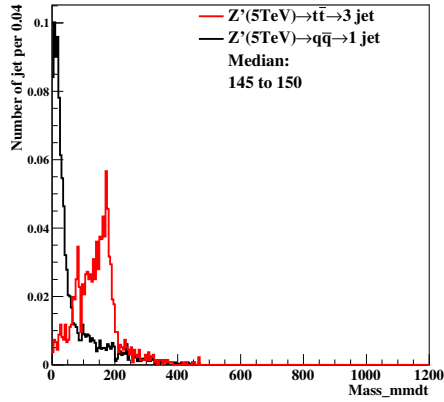
(b) 10TeV at 20×20 (cm \times cm) in cluster



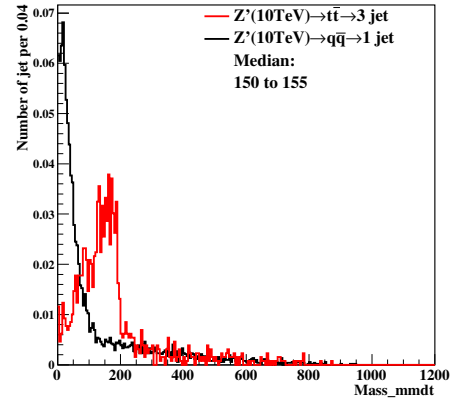
(c) 5TeV at 5×5 (cm \times cm) in cluster



(d) 10TeV at 5×5 (cm \times cm) in cluster

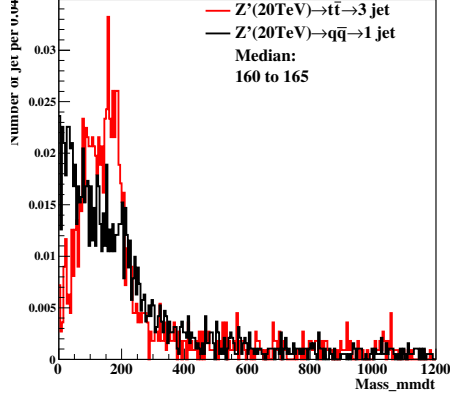


(e) 5TeV at 1×1 (cm \times cm) in cluster

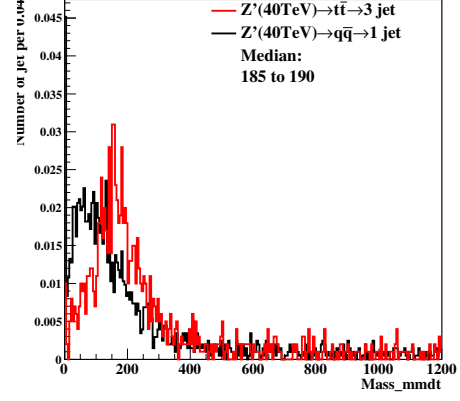


(f) 10TeV at 1×1 (cm \times cm) in cluster

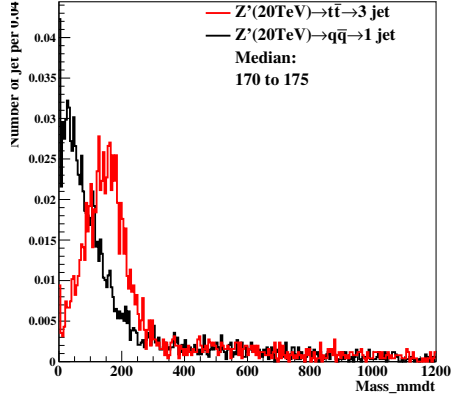
Figure 4: Distributions of mass soft drop at $\beta=0$, signal= tt , in 5,10TeV energy of collision in different detector sizes. Cell Size in 20×20 , 5×5 , and 1×1 (cm \times cm) are shown here.



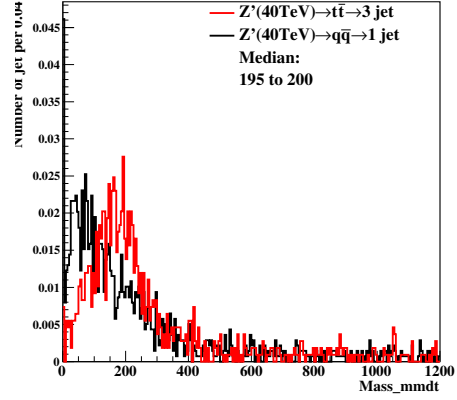
(a) 20TeV at 20×20(cm×cm) in cluster



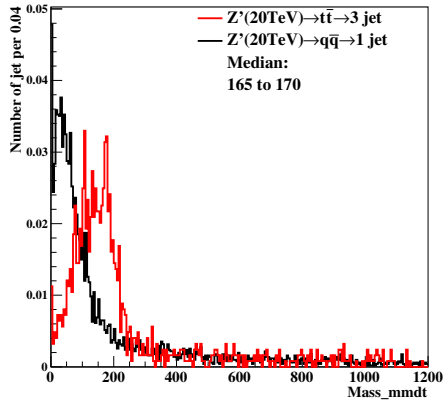
(b) 40TeV at 20×20(cm×cm) in cluster



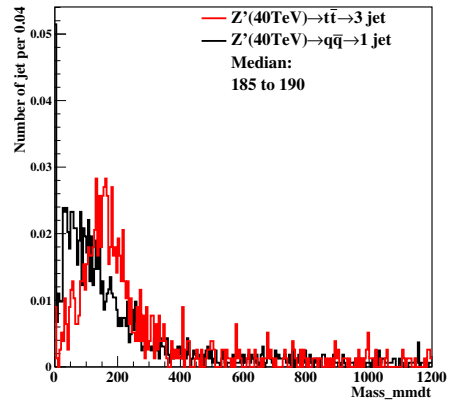
(c) 20TeV at 5×5(cm×cm) in cluster



(d) 40TeV at 5×5(cm×cm) in cluster

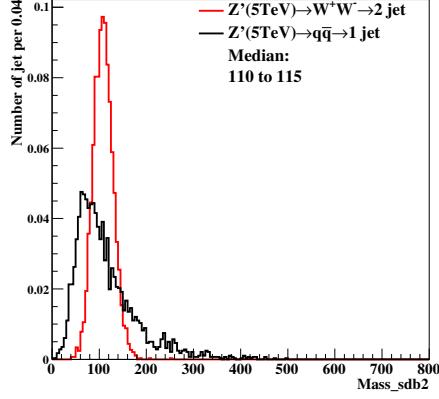


(e) 20TeV at 1×1(cm×cm) in cluster

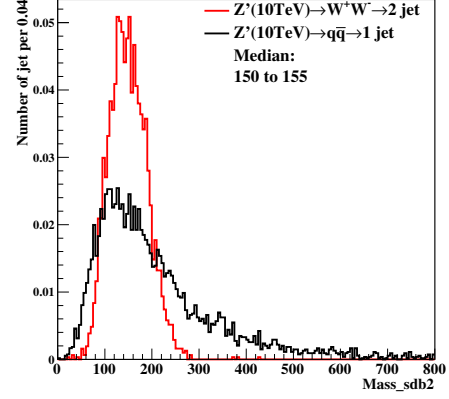


(f) 40TeV at 1×1(cm×cm) in cluster

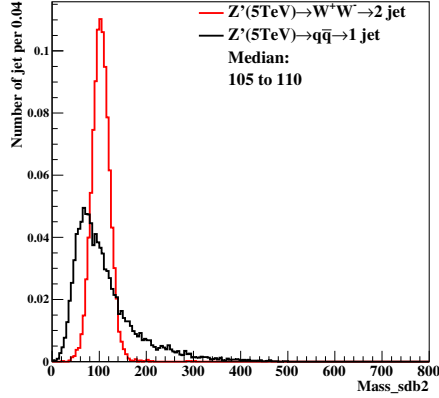
Figure 5: Distributions of mass soft drop at $\beta=0$, signal= $t\bar{t}$, in 20,40TeV energy of collision in different detector sizes. Cell Size in 20×20, 5×5, and 1×1(cm×cm) are shown here.



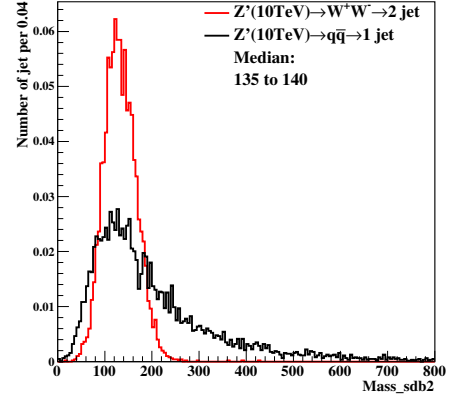
(a) 5TeV at 20×20(cm×cm) in cluster



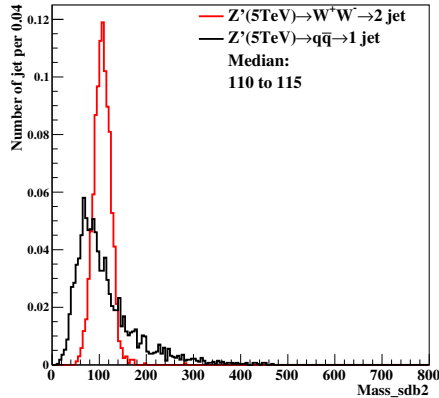
(b) 10TeV at 20×20(cm×cm) in cluster



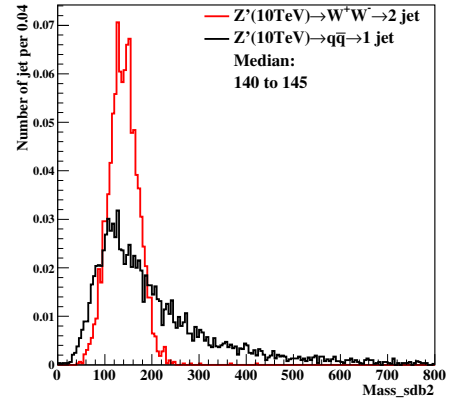
(c) 5TeV at 5×5(cm×cm) in cluster



(d) 10TeV at 5×5(cm×cm) in cluster

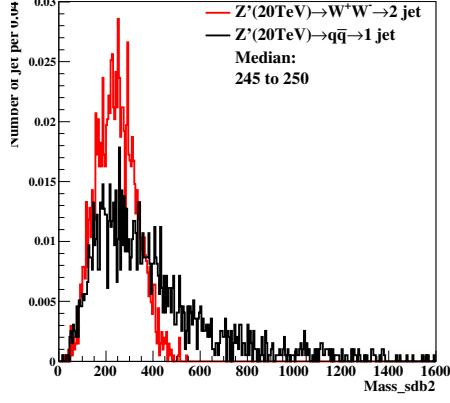


(e) 5TeV at 1×1(cm×cm) in cluster

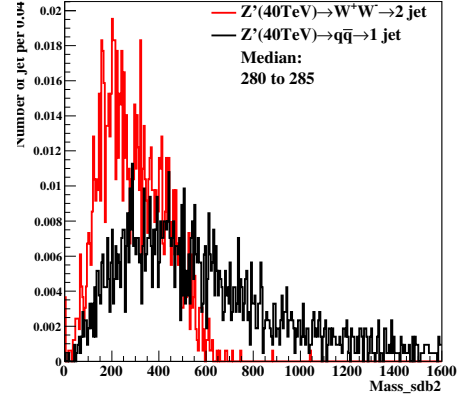


(f) 10TeV at 1×1(cm×cm) in cluster

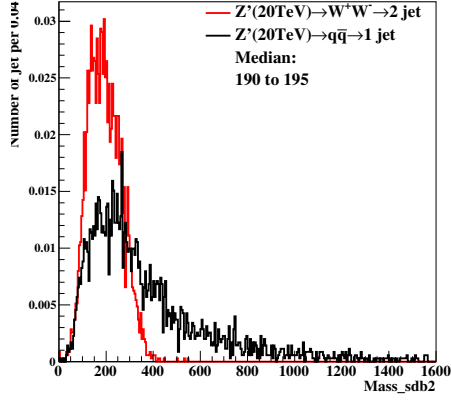
Figure 6: Distributions of mass soft drop at $\beta=2$, signal=ww, in 5,10TeV energy of collision in different detector sizes. Cell Size in 20×20, 5×5, and 1×1(cm×cm) are shown here.



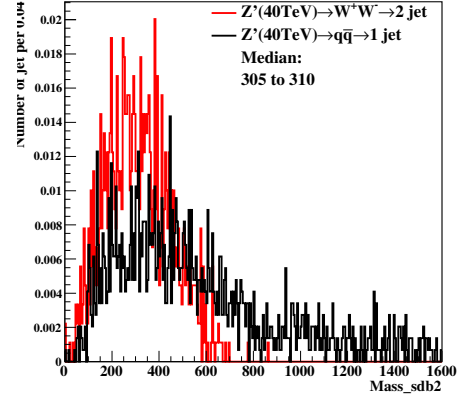
(a) 20TeV at 20×20(cm×cm) in cluster



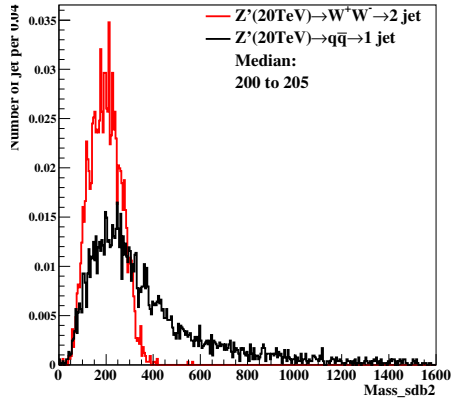
(b) 40TeV at 20×20(cm×cm) in cluster



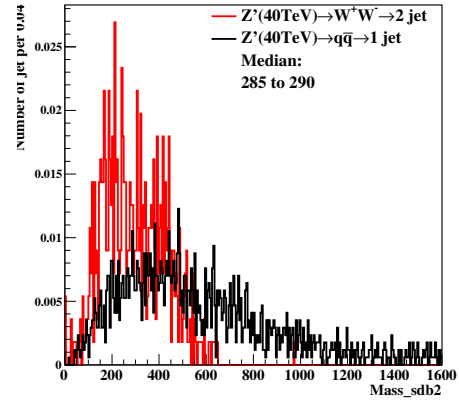
(c) 20TeV at 5×5(cm×cm) in cluster



(d) 40TeV at 5×5(cm×cm) in cluster

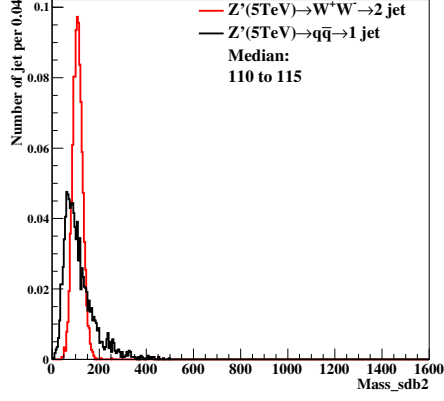


(e) 20TeV at 1×1(cm×cm) in cluster

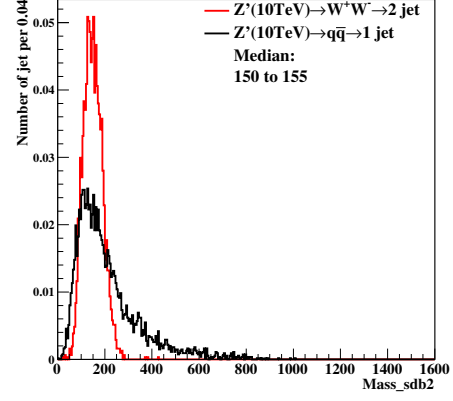


(f) 40TeV at 1×1(cm×cm) in cluster

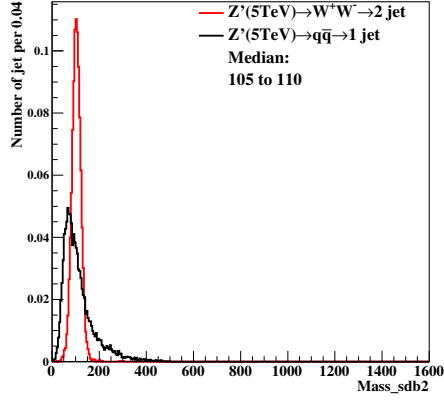
Figure 7: Distributions of mass soft drop at $\beta=2$, signal=ww, in 20,40TeV energy of collision in different detector sizes. Cell Size in 20×20, 5×5, and 1×1(cm×cm) are shown here.



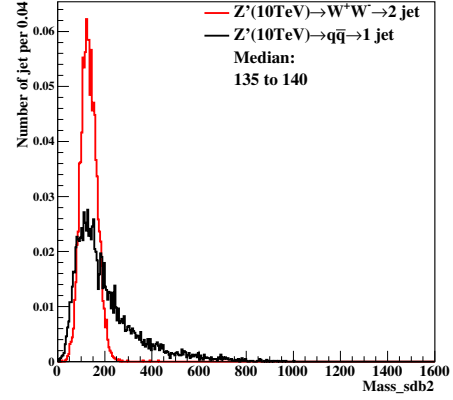
(a) 5TeV at 20×20 (cm \times cm) in cluster



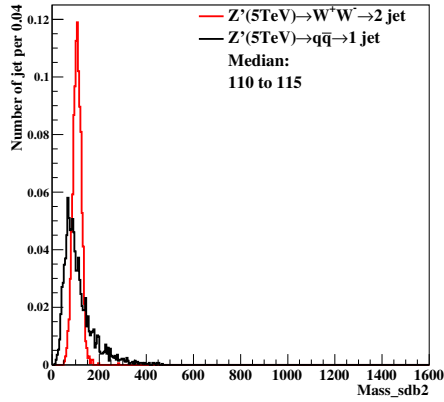
(b) 10TeV at 20×20 (cm \times cm) in cluster



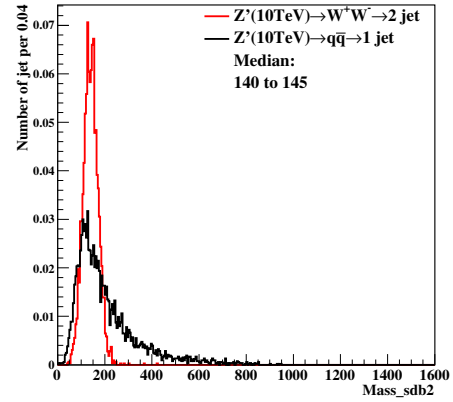
(c) 5TeV at 5×5 (cm \times cm) in cluster



(d) 10TeV at 5×5 (cm \times cm) in cluster



(e) 5TeV at 1×1 (cm \times cm) in cluster



(f) 10TeV at 1×1 (cm \times cm) in cluster

Figure 8: Distributions of mass soft drop at $\beta=2$, signal=ww, in 5,10TeV energy of collision in different detector sizes. Cell Size in 20×20 , 5×5 , and 1×1 (cm \times cm) are shown here.

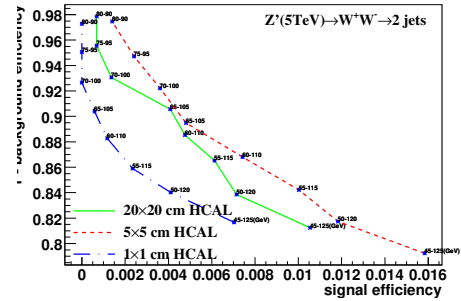


Figure 10 is a plot showing the 1% constant efficiency signal efficiency versus the signal efficiency for the $Z'(5\text{TeV}) \rightarrow W^+W^- \rightarrow 2 \text{ jets}$ process. The plot compares three HCAL configurations: 20x20 cm (solid green line), 5x5 cm (dashed red line), and 1x1 cm (dashed blue line). Data points are labeled with their corresponding signal efficiencies and constant efficiencies. The 1x1 cm HCAL configuration shows the highest signal efficiency for a given constant efficiency, while the 20x20 cm configuration shows the lowest.

HCAL Configuration	Signal Efficiency	1% Constant Efficiency
20x20 cm	0.0015	0.965
20x20 cm	0.0025	0.945
20x20 cm	0.0035	0.925
20x20 cm	0.0045	0.905
20x20 cm	0.0055	0.885
20x20 cm	0.0065	0.865
20x20 cm	0.0075	0.845
20x20 cm	0.0085	0.825
20x20 cm	0.0095	0.805
20x20 cm	0.0105	0.785
20x20 cm	0.0115	0.765
20x20 cm	0.0125	0.745
20x20 cm	0.0135	0.725
20x20 cm	0.0145	0.705
20x20 cm	0.0155	0.685
20x20 cm	0.0165	0.665
20x20 cm	0.0175	0.645
20x20 cm	0.0185	0.625
20x20 cm	0.0195	0.605
20x20 cm	0.0205	0.585
20x20 cm	0.0215	0.565
20x20 cm	0.0225	0.545
20x20 cm	0.0235	0.525
20x20 cm	0.0245	0.505
20x20 cm	0.0255	0.485
20x20 cm	0.0265	0.465
20x20 cm	0.0275	0.445
20x20 cm	0.0285	0.425
20x20 cm	0.0295	0.405
20x20 cm	0.0305	0.385
20x20 cm	0.0315	0.365
20x20 cm	0.0325	0.345
20x20 cm	0.0335	0.325
20x20 cm	0.0345	0.305
20x20 cm	0.0355	0.285
20x20 cm	0.0365	0.265
20x20 cm	0.0375	0.245
20x20 cm	0.0385	0.225
20x20 cm	0.0395	0.205
20x20 cm	0.0405	0.185
20x20 cm	0.0415	0.165
20x20 cm	0.0425	0.145
20x20 cm	0.0435	0.125
20x20 cm	0.0445	0.105
20x20 cm	0.0455	0.085
20x20 cm	0.0465	0.065
20x20 cm	0.0475	0.045
20x20 cm	0.0485	0.025
20x20 cm	0.0495	0.005
20x20 cm	0.0505	0.000
5x5 cm	0.0015	0.965
5x5 cm	0.0025	0.945
5x5 cm	0.0035	0.925
5x5 cm	0.0045	0.905
5x5 cm	0.0055	0.885
5x5 cm	0.0065	0.865
5x5 cm	0.0075	0.845
5x5 cm	0.0085	0.825
5x5 cm	0.0095	0.805
5x5 cm	0.0105	0.785
5x5 cm	0.0115	0.765
5x5 cm	0.0125	0.745
5x5 cm	0.0135	0.725
5x5 cm	0.0145	0.705
5x5 cm	0.0155	0.685
5x5 cm	0.0165	0.665
5x5 cm	0.0175	0.645
5x5 cm	0.0185	0.625
5x5 cm	0.0195	0.605
5x5 cm	0.0205	0.585
5x5 cm	0.0215	0.565
5x5 cm	0.0225	0.545
5x5 cm	0.0235	0.525
5x5 cm	0.0245	0.505
5x5 cm	0.0255	0.485
5x5 cm	0.0265	0.465
5x5 cm	0.0275	0.445
5x5 cm	0.0285	0.425
5x5 cm	0.0295	0.405
5x5 cm	0.0305	0.385
5x5 cm	0.0315	0.365
5x5 cm	0.0325	0.345
5x5 cm	0.0335	0.325
5x5 cm	0.0345	0.305
5x5 cm	0.0355	0.285
5x5 cm	0.0365	0.265
5x5 cm	0.0375	0.245
5x5 cm	0.0385	0.225
5x5 cm	0.0395	0.205
5x5 cm	0.0405	0.185
5x5 cm	0.0415	0.165
5x5 cm	0.0425	

Figure 1 is a plot showing the Z' branching ratio into two jets, $BR(Z' \rightarrow W^+W^- \rightarrow 2 \text{ jets})$, as a function of the signal efficiency for three different detector configurations: 20×20 cm HCAL (solid green line), 5×5 cm HCAL (dashed red line), and 1×1 cm HCAL (dashed blue line). The y-axis represents the branching ratio, ranging from 0.75 to 0.95. The x-axis represents the signal efficiency, ranging from 0 to 0.035. Data points are labeled with p_T values: $p_T=105$, $p_T=110$, $p_T=115$, $p_T=120$, $p_T=125$, $p_T=130$, $p_T=135$, and $p_T=140$ (GeV). The branching ratio decreases as the signal efficiency increases and as the HCAL size decreases.

Figure 10 is a plot showing the 1-2 angular distribution efficiency versus signal efficiency for the $Z'(5\text{TeV}) \rightarrow W^+W^- \rightarrow 2 \text{ jets}$ process. The plot compares three HCAL configurations: 20x20 cm (solid green line), 5x5 cm (dashed red line), and 1x1 cm (dashed blue line). The x-axis represents signal efficiency from 0 to 0.06, and the y-axis represents 1-2 angular distribution efficiency from 0.7 to 0.95. Data points are labeled with their corresponding signal efficiencies.

Signal Efficiency	20x20 cm HCAL	5x5 cm HCAL	1x1 cm HCAL
0.005	0.95	0.95	0.95
0.01	0.93	0.93	0.93
0.015	0.91	0.91	0.91
0.02	0.89	0.89	0.89
0.025	0.87	0.87	0.87
0.03	0.85	0.85	0.85
0.035	0.83	0.83	0.83
0.04	0.81	0.81	0.81
0.045	0.79	0.79	0.79
0.05	0.77	0.77	0.77
0.055	0.75	0.75	0.75
0.06	0.73	0.73	0.73

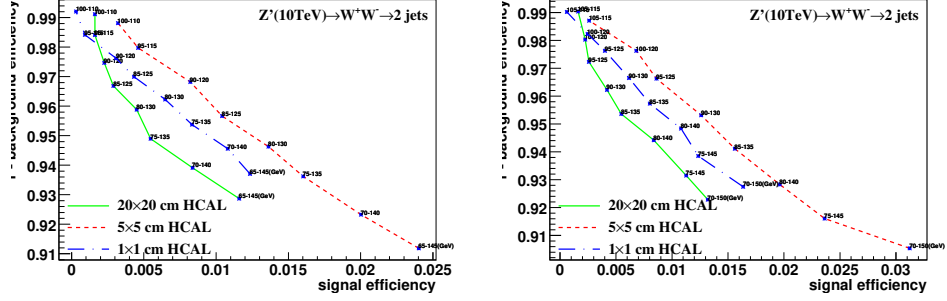
Figure 10 is a plot showing the Z' branching ratio efficiency (Y-axis, ranging from 0.7 to 0.95) versus the signal efficiency (X-axis, ranging from 0 to 0.08). The plot is titled $Z'(5\text{TeV}) \rightarrow W^+W^- \rightarrow 2 \text{ jets}$. Three curves are shown, corresponding to different HCAL cell sizes:

- $20 \times 20 \text{ cm HCAL}$ (solid green line)
- $5 \times 5 \text{ cm HCAL}$ (dashed red line)
- $1 \times 1 \text{ cm HCAL}$ (dashed blue line)

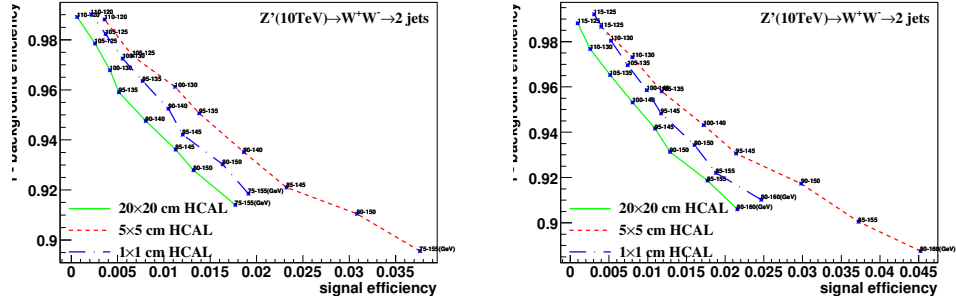
The curves show that the branching ratio efficiency decreases as the signal efficiency increases, and that the efficiency is highest for the smallest HCAL cell size ($1 \times 1 \text{ cm}$) and lowest for the largest cell size ($20 \times 20 \text{ cm}$). Data points on the curves are labeled with p_T values (e.g., $p_T=120$, $p_T=130$, etc.).

(g) Central at 110TeV change width in cluster (h) Central at 115TeV change width in cluster

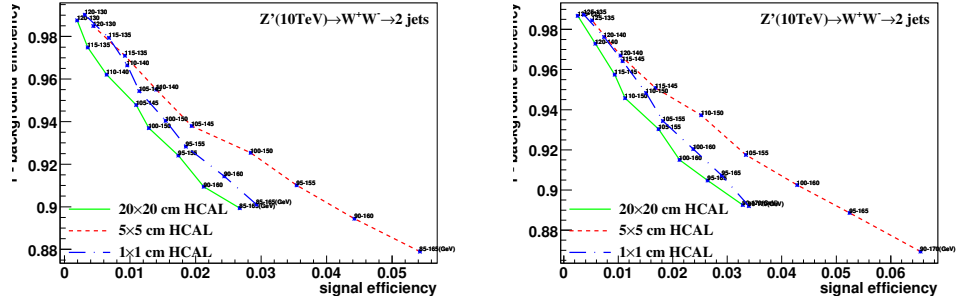
Figure 9: study of "fix central and change width" in mass soft drop at $\beta=2$, signal=ww, in 5TeV energy of collision in different detector sizes. Cell Size in 20×20 , 5×5 , and 1×1 (cm \times cm) are shown in each picture.



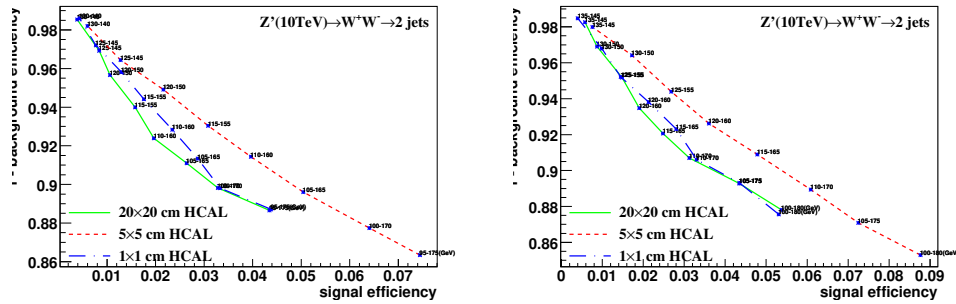
(a) Central at 105TeV change width in cluster (b) Central at 110TeV change width in cluster



(c) Central at 115TeV change width in cluster (d) Central at 120TeV change width in cluster

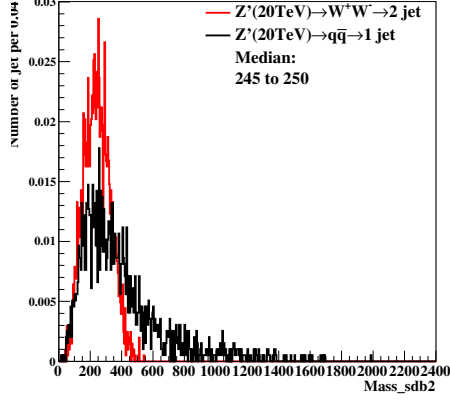


(e) Central at 125TeV change width in cluster (f) Central at 130TeV change width in cluster

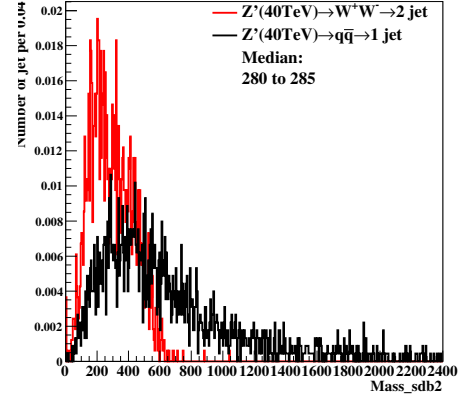


(g) Central at 135TeV change width in cluster (h) Central at 140TeV change width in cluster

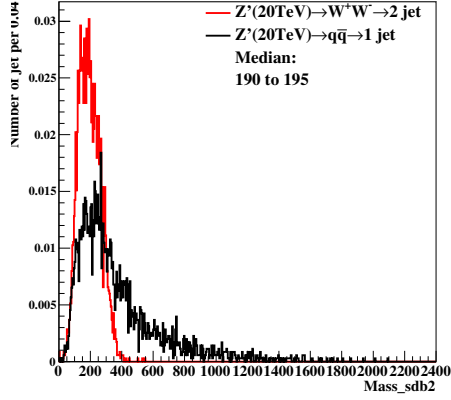
Figure 10: study of "fix central and change width" in mass soft drop at $\beta=2$, signal=ww, in 10TeV energy of collision in different detector sizes. Cell Size in 20x20, 5x5, and 1x1(cm x cm) are shown in each picture.



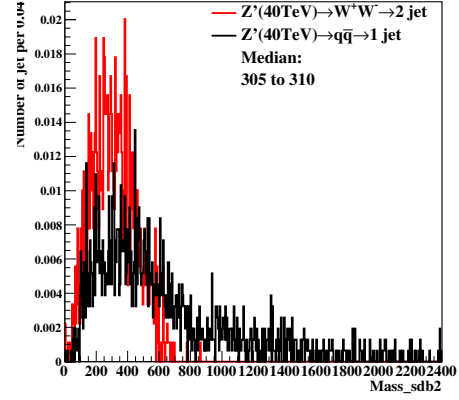
(a) 20TeV at 20×20(cm×cm) in cluster



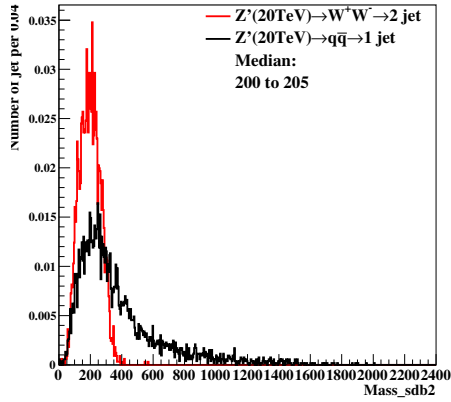
(b) 40TeV at 20×20(cm×cm) in cluster



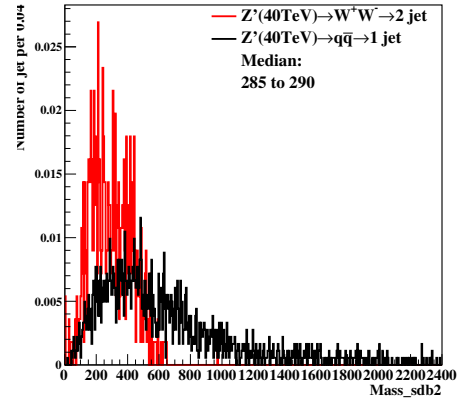
(c) 20TeV at 5×5(cm×cm) in cluster



(d) 40TeV at 5×5(cm×cm) in cluster

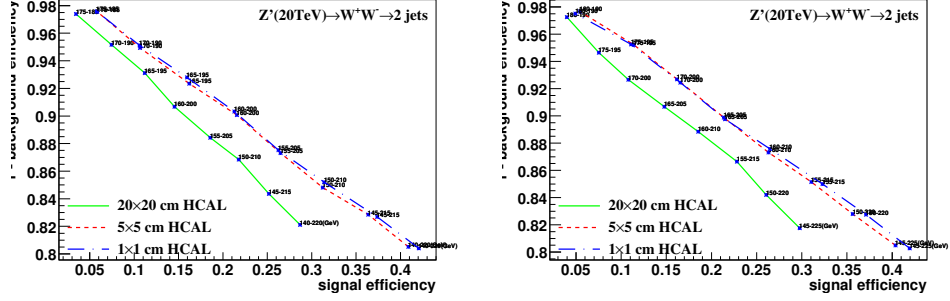


(e) 20TeV at 1×1(cm×cm) in cluster

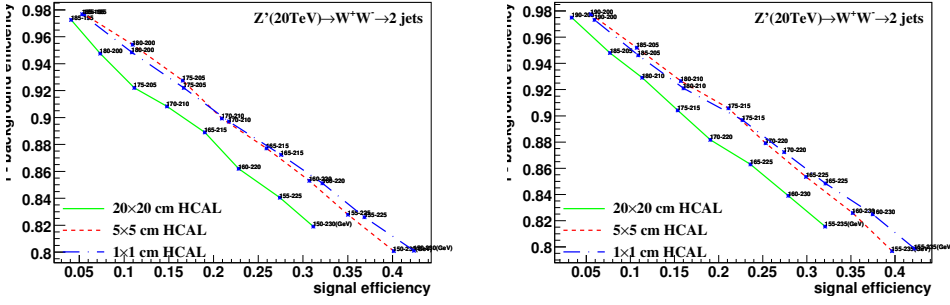


(f) 40TeV at 1×1(cm×cm) in cluster

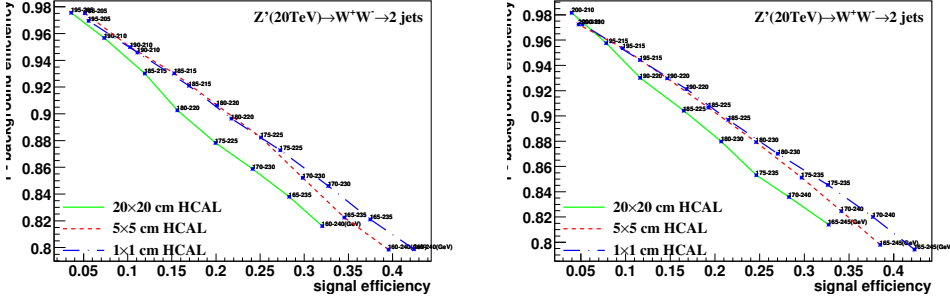
Figure 11: Distributions of mass soft drop at $\beta=2$, signal=ww, in 20,40TeV energy of collision in different detector sizes. Cell Size in 20×20, 5×5, and 1×1(cm×cm) are shown here.



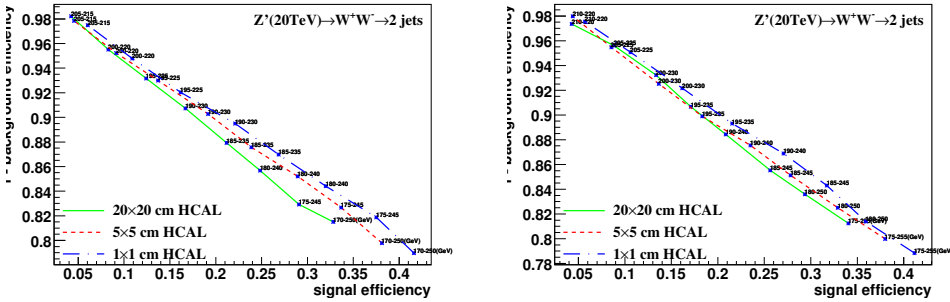
(a) Central at 180TeV change width in cluster (b) Central at 185TeV change width in cluster



(c) Central at 190TeV change width in cluster (d) Central at 195TeV change width in cluster

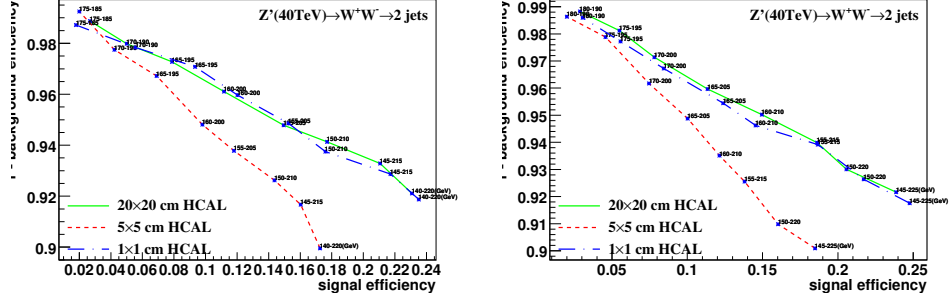


(e) Central at 200TeV change width in cluster (f) Central at 205TeV change width in cluster

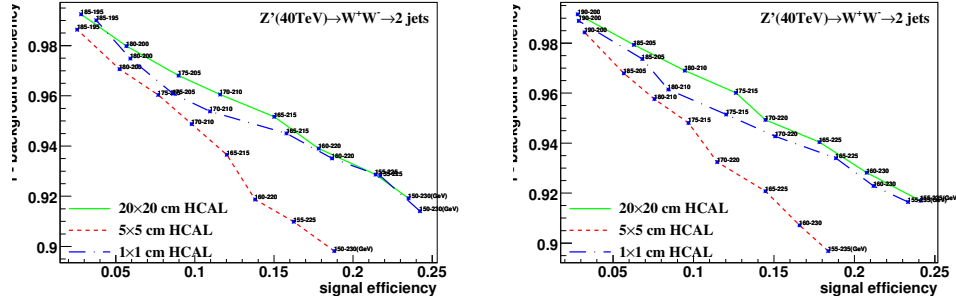


(g) Central at 210TeV change width in cluster (h) Central at 215TeV change width in cluster

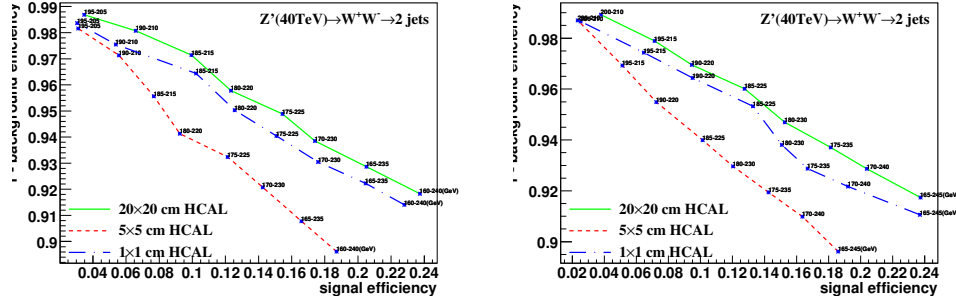
Figure 12: study of "fix central and change width" in mass soft drop at $\beta=2$, signal=ww, in 20TeV energy of collision in different detector sizes. Cell Size in 20x20, 5x5, and 1x1(cm x cm) are shown in each picture.



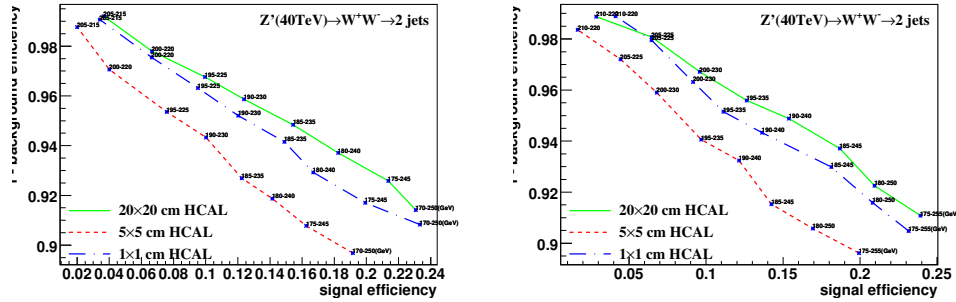
(a) Central at 180TeV change width in cluster (b) Central at 185TeV change width in cluster



(c) Central at 190TeV change width in cluster (d) Central at 195TeV change width in cluster

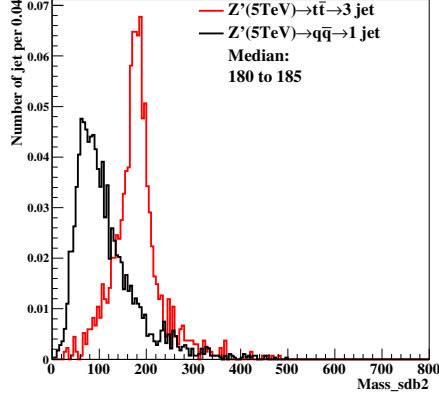


(e) Central at 200TeV change width in cluster (f) Central at 205TeV change width in cluster

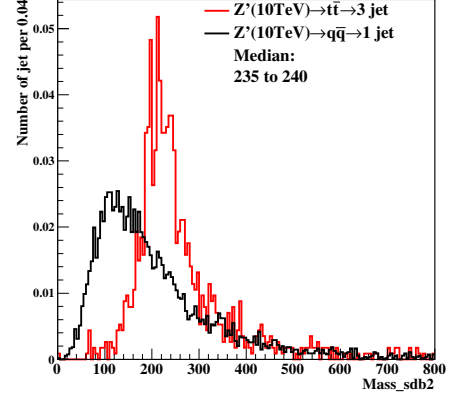


(g) Central at 210TeV change width in cluster (h) Central at 215TeV change width in cluster

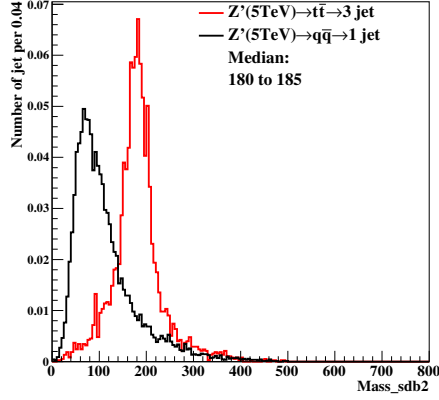
Figure 13: study of "fix central and change width" in mass soft drop at $\beta=2$, signal=ww, in 40TeV energy of collision in different detector sizes. Cell Size in 20x20, 5x5, and 1x1(cm x cm) are shown in each picture.



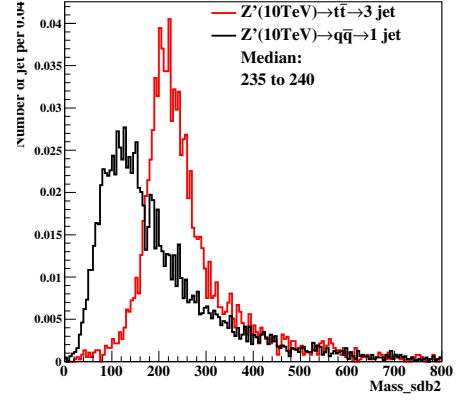
(a) 5TeV at 20×20(cm×cm) in cluster



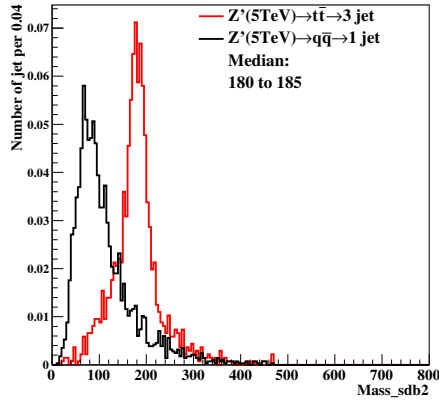
(b) 10TeV at 20×20(cm×cm) in cluster



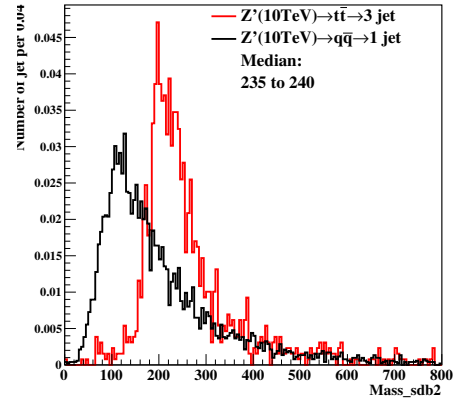
(c) 5TeV at 5×5(cm×cm) in cluster



(d) 10TeV at 5×5(cm×cm) in cluster

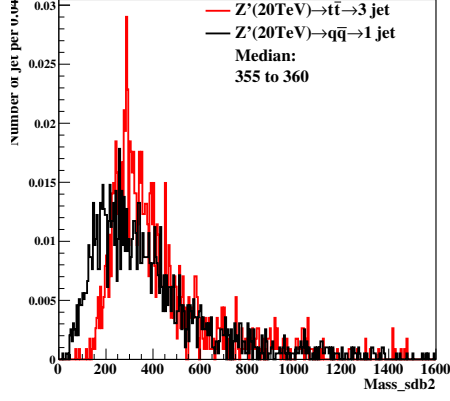


(e) 5TeV at 1×1(cm×cm) in cluster

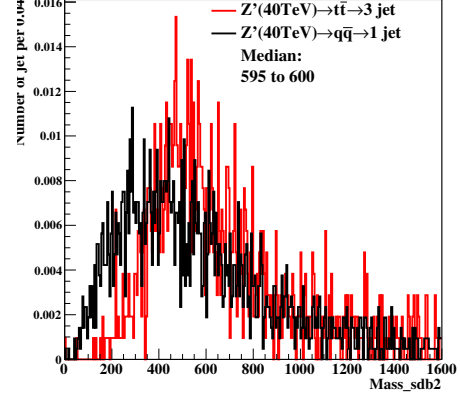


(f) 10TeV at 1×1(cm×cm) in cluster

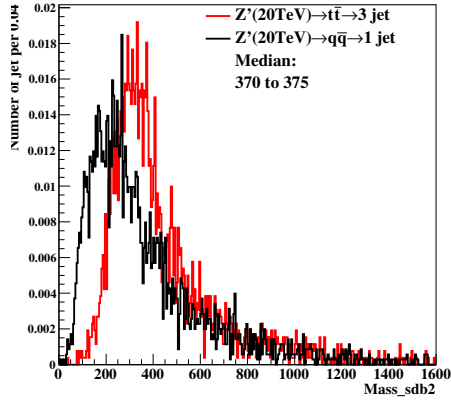
Figure 14: Distributions of mass soft drop at $\beta=2$, signal= tt , in 5,10TeV energy of collision in different detector sizes. Cell Size in 20×20, 5×5, and 1×1(cm×cm) are shown here.



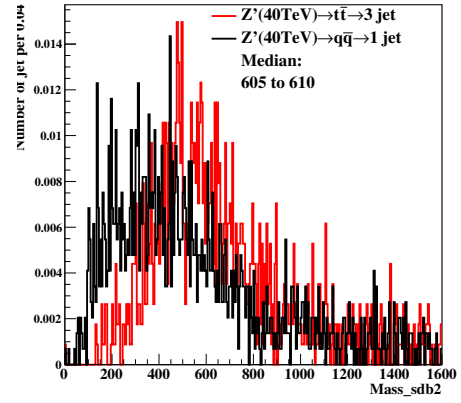
(a) 20TeV at 20×20(cm×cm) in cluster



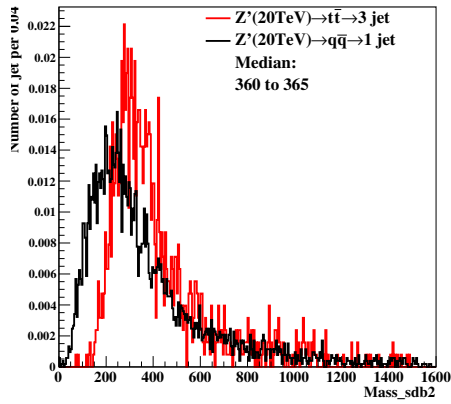
(b) 40TeV at 20×20(cm×cm) in cluster



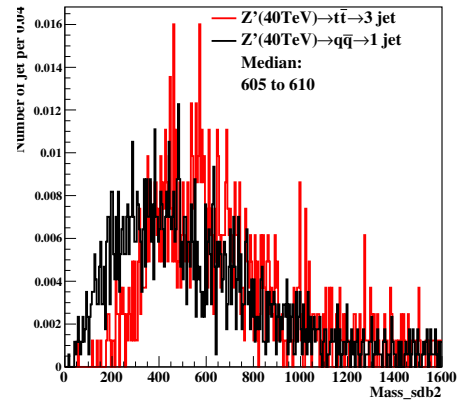
(c) 20TeV at 5×5(cm×cm) in cluster



(d) 40TeV at 5×5(cm×cm) in cluster

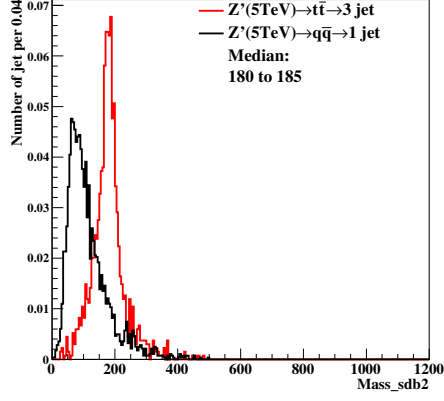


(e) 20TeV at 1×1(cm×cm) in cluster

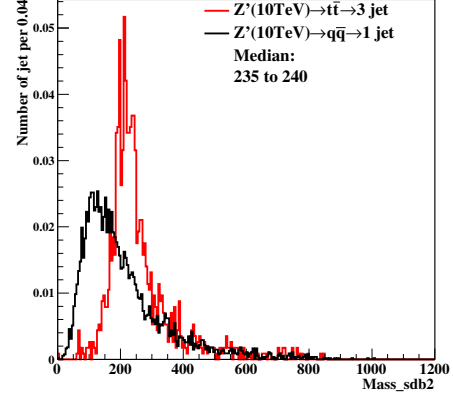


(f) 40TeV at 1×1(cm×cm) in cluster

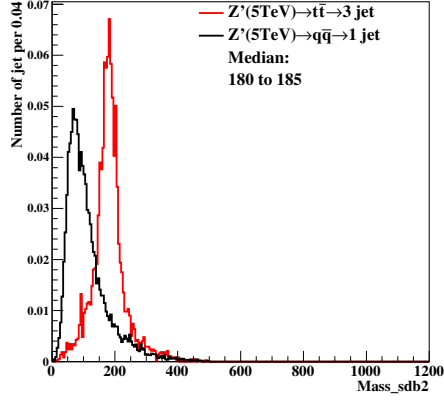
Figure 15: Distributions of mass soft drop at $\beta=2$, signal= $t\bar{t}$, in 20,40TeV energy of collision in different detector sizes. Cell Size in 20×20, 5×5, and 1×1(cm×cm) are shown here.



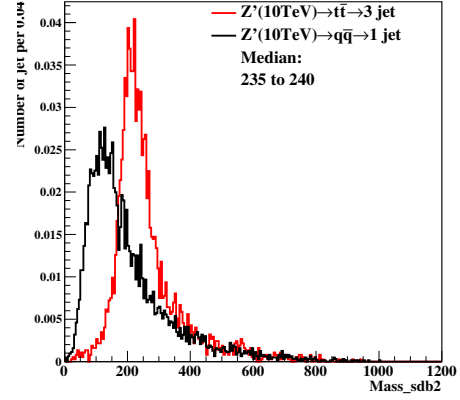
(a) 5TeV at 20×20 (cm \times cm) in cluster



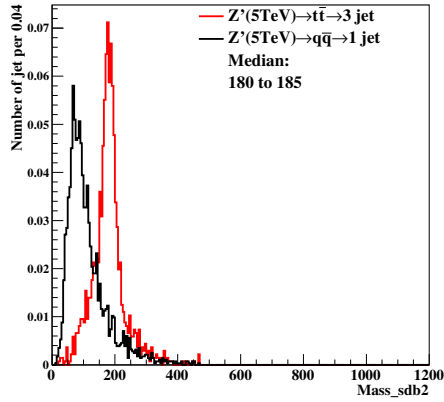
(b) 10TeV at 20×20 (cm \times cm) in cluster



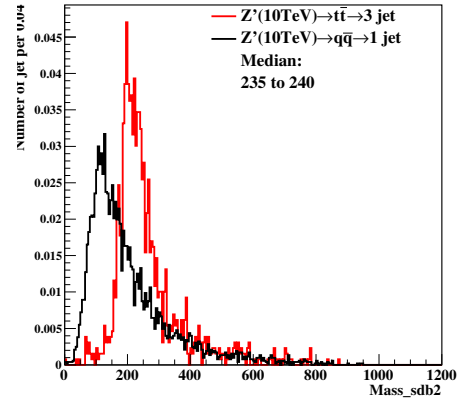
(c) 5TeV at 5×5 (cm \times cm) in cluster



(d) 10TeV at 5×5 (cm \times cm) in cluster

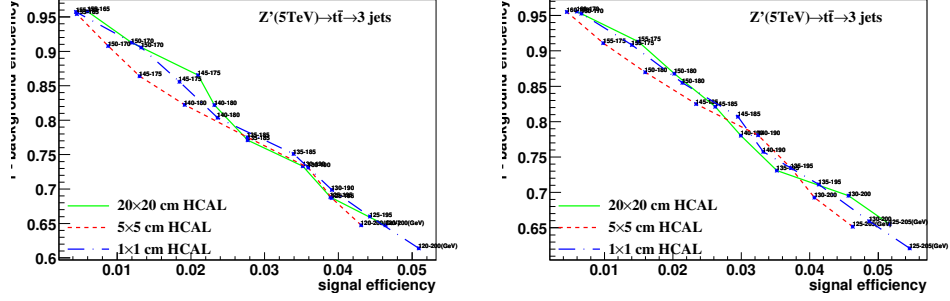


(e) 5TeV at 1×1 (cm \times cm) in cluster

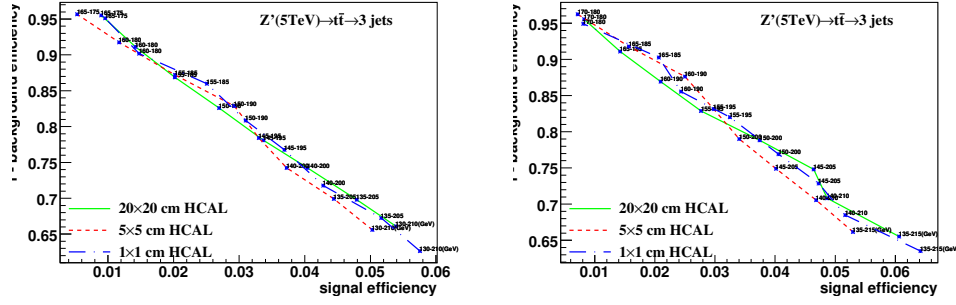


(f) 10TeV at 1×1 (cm \times cm) in cluster

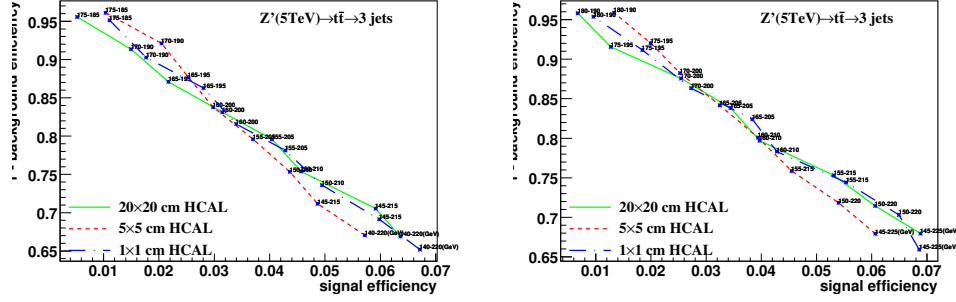
Figure 16: Distributions of mass soft drop at $\beta=2$, signal= tt , in 5,10TeV energy of collision in different detector sizes. Cell Size in 20×20 , 5×5 , and 1×1 (cm \times cm) are shown here.



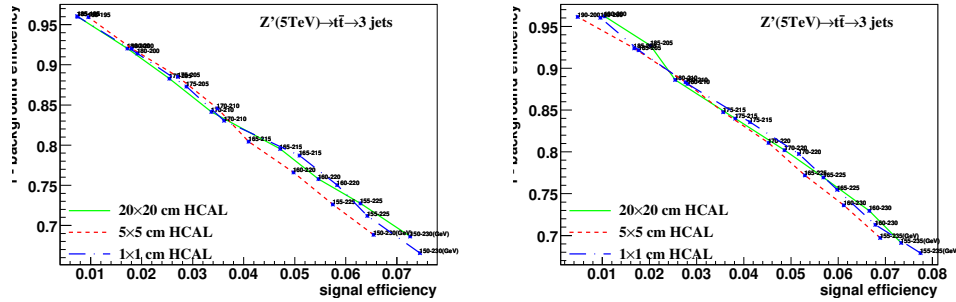
(a) Central at 160TeV change width in cluster (b) Central at 165TeV change width in cluster



(c) Central at 170TeV change width in cluster (d) Central at 175TeV change width in cluster

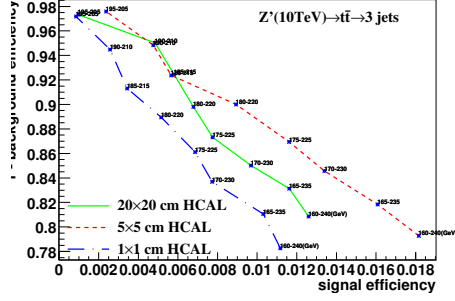


(e) Central at 180TeV change width in cluster (f) Central at 185TeV change width in cluster

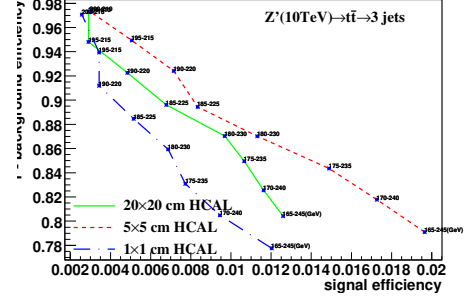


(g) Central at 190TeV change width in cluster (h) Central at 195TeV change width in cluster

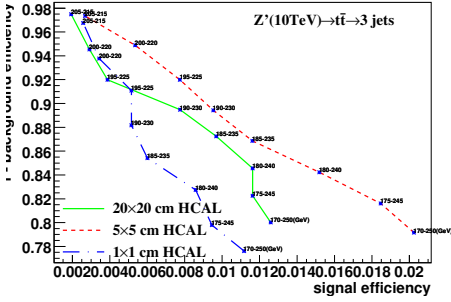
Figure 17: study of "fix central and change width" in mass soft drop at $\beta=2$, signal=tt, in 5TeV energy of collision in different detector sizes. Cell Size in 20×20 , 5×5 , and 1×1 (cm \times cm) are shown in each picture.



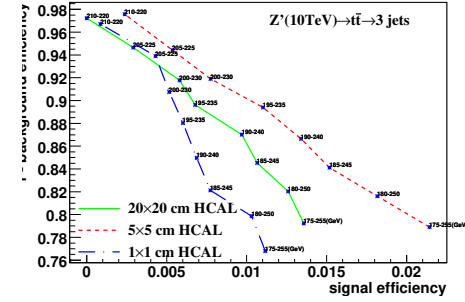
(a) Central at 200TeV change width in cluster



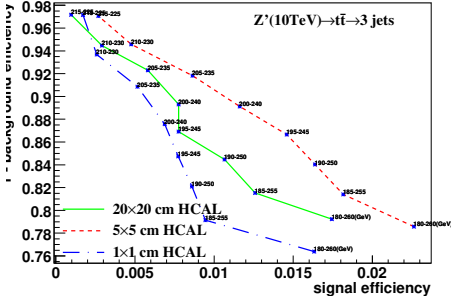
(b) Central at 205TeV change width in cluster



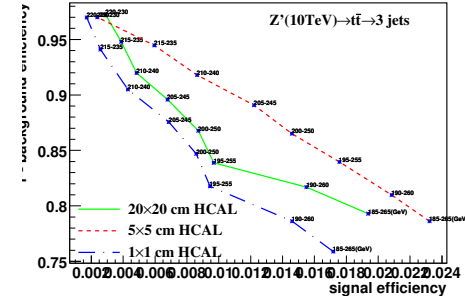
(c) Central at 210TeV change width in cluster



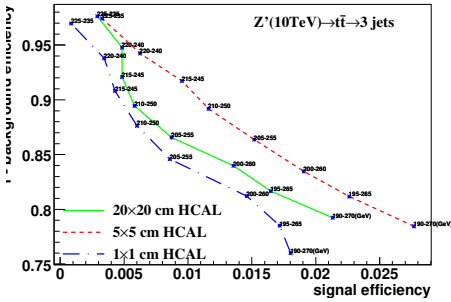
(d) Central at 215TeV change width in cluster



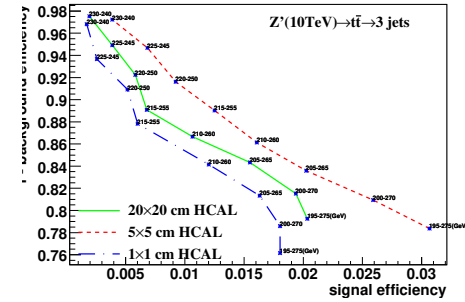
(e) Central at 220TeV change width in cluster



(f) Central at 225TeV change width in cluster

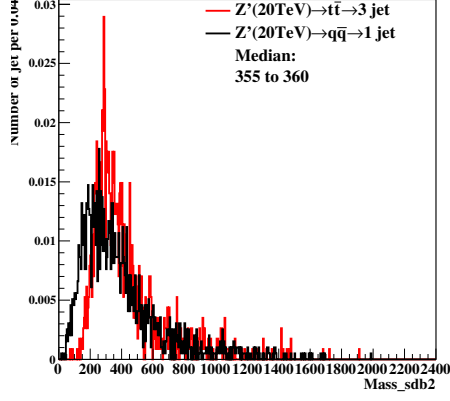


(g) Central at 230TeV change width in cluster

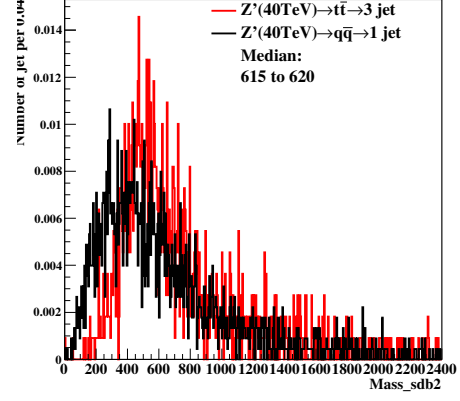


(h) Central at 235TeV change width in cluster

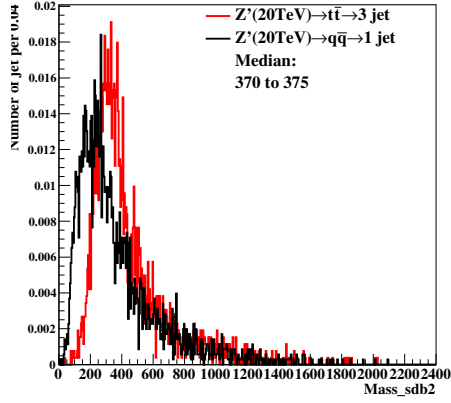
Figure 18: study of "fix central and change width" in mass soft drop at $\beta=2$, signal= $t\bar{t}$, in 10TeV energy of collision in different detector sizes. Cell Size in 20×20 , 5×5 , and 1×1 (cm \times cm) are shown in each picture.



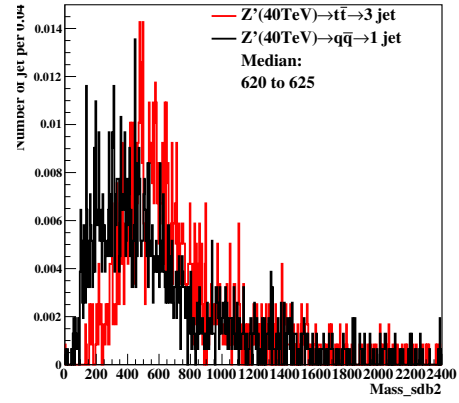
(a) 20TeV at 20×20(cm×cm) in cluster



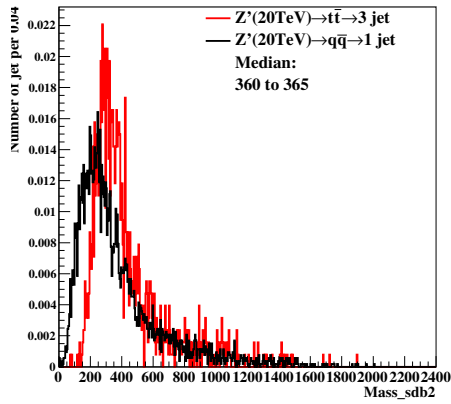
(b) 40TeV at 20×20(cm×cm) in cluster



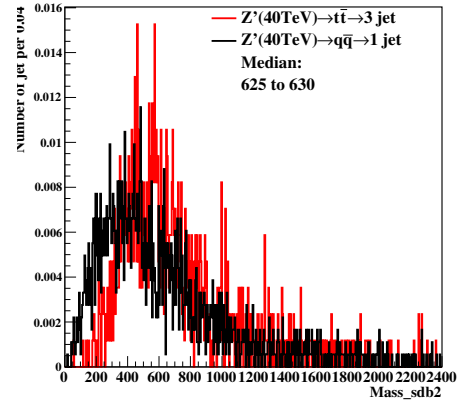
(c) 20TeV at 5×5(cm×cm) in cluster



(d) 40TeV at 5×5(cm×cm) in cluster

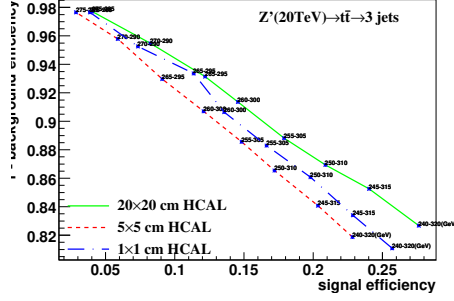


(e) 20TeV at 1×1(cm×cm) in cluster

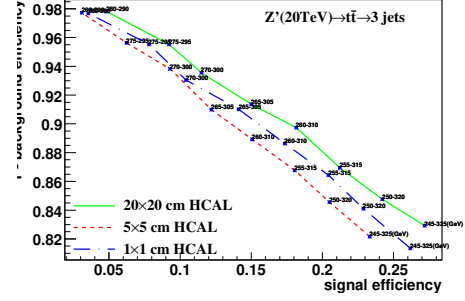


(f) 40TeV at 1×1(cm×cm) in cluster

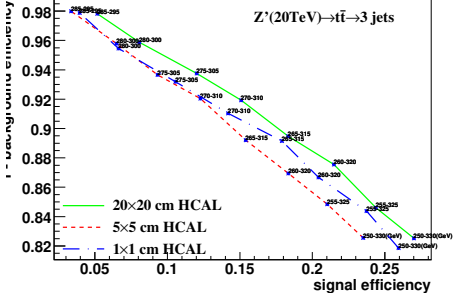
Figure 19: Distributions of mass soft drop at $\beta=2$, signal= $t\bar{t}$, in 20,40TeV energy of collision in different detector sizes. Cell Size in 20×20, 5×5, and 1×1(cm×cm) are shown here.



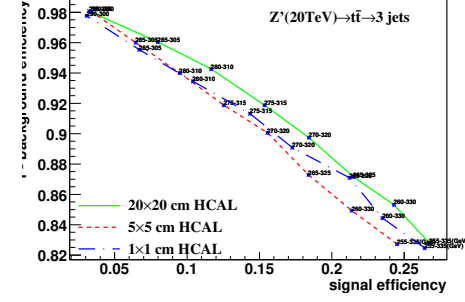
(a) Central at 280TeV change width in cluster



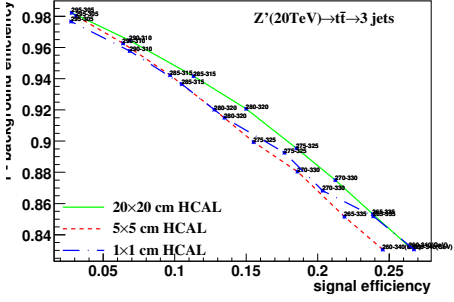
(b) Central at 285TeV change width in cluster



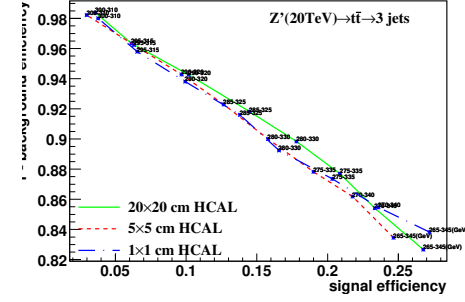
(c) Central at 290TeV change width in cluster



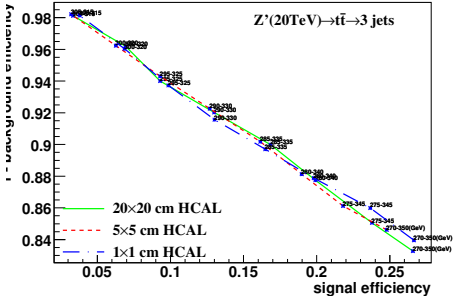
(d) Central at 295TeV change width in cluster



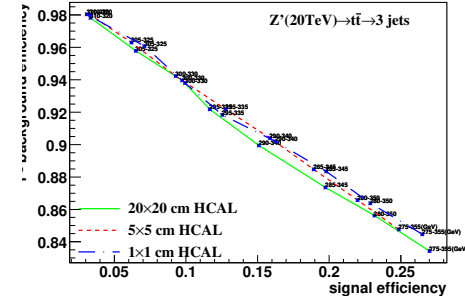
(e) Central at 300TeV change width in cluster



(f) Central at 305TeV change width in cluster

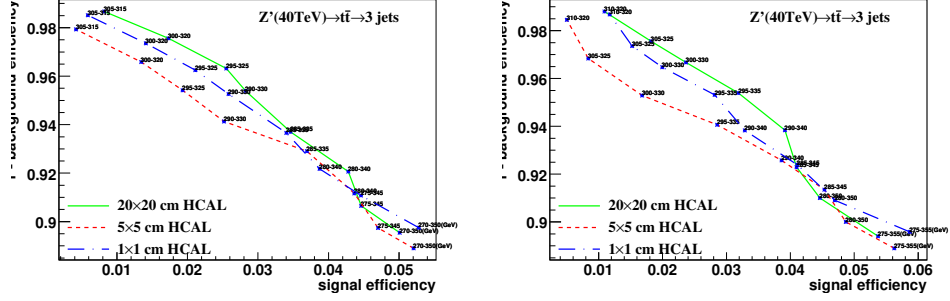


(g) Central at 310TeV change width in cluster

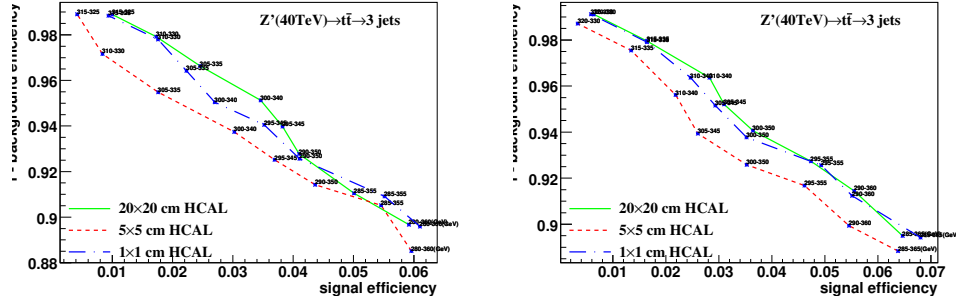


(h) Central at 315TeV change width in cluster

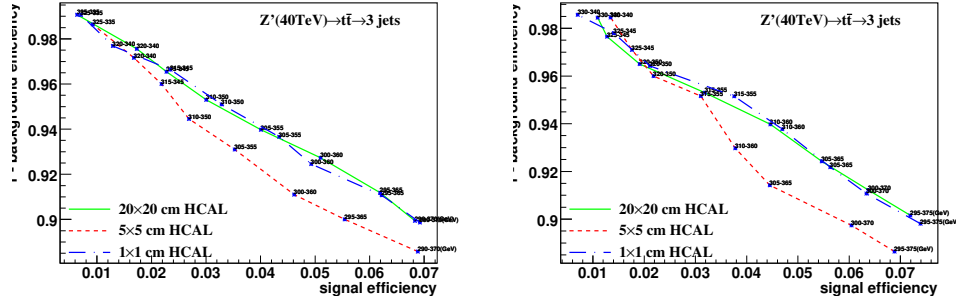
Figure 20: study of "fix central and change width" in mass soft drop at $\beta=2$, signal= $t\bar{t}$, in 20TeV energy of collision in different detector sizes. Cell Size in 20×20 , 5×5 , and 1×1 (cm \times cm) are shown in each picture.



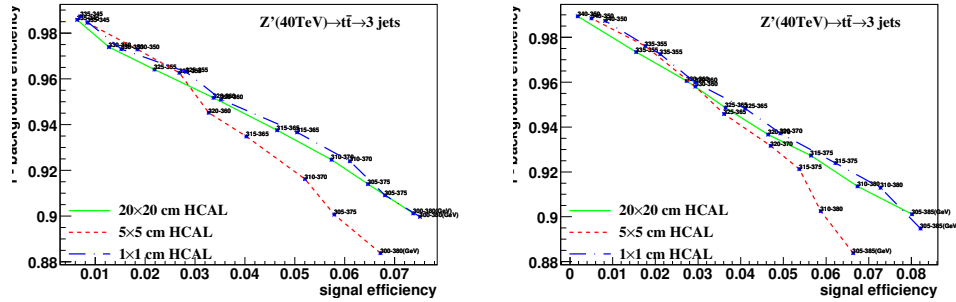
(a) Central at 310TeV change width in clus- (b) Central at 315TeV change width in cluster



(c) Central at 320TeV change width in cluster (d) Central at 325TeV change width in cluster



(e) Central at 330TeV change width in cluster (f) Central at 335TeV change width in cluster



(g) Central at 340TeV change width in cluster (h) Central at 345TeV change width in cluster

Figure 21: study of "fix central and change width" in mass soft drop at $\beta=2$, signal= $t\bar{t}$, in 40TeV energy of collision in different detector sizes. Cell Size in 20×20 , 5×5 , and 1×1 (cm \times cm) are shown in each picture.